Published in final edited form as:
Neuroimage. 2013 October ; 79: 62–71. doi:10.1016/j.neuroimage.2013.04.038.

Task-related concurrent but opposite modulations of overlapping functional networks as revealed by spatial ICA

Jiansong Xu[1,*], **Sheng Zhang**[1], **Vince D. Calhoun**[1,5,7], **John Monterosso**[4], **Chiang-Shan R. Li**[1,3], **Patrick D. Worhunsky**[1], **Michael Stevens**[1,6], **Godfrey D. Pearlson**[1,3,6], and **Marc N. Potenza**[1,2,3]

[1]Department of Psychiatry, Yale University School of Medicine, New Haven, CT 06510, United States

[2]Child Study Center, Yale University School of Medicine, New Haven, CT 06510, United States

[3]Department of Neurobiology, Yale University School of Medicine, New Haven, CT 06510, United States

[4]Department of Psychology, University of Southern California, Los Angeles, CA 90033, United States

[5]The Mind Research Network, Albuquerque, NM 87131, United States

[6]Olin Neuropsychiatry Research Center, Institute of Living, Hartford, Connecticut, CT 06106, United States

[7]Dept of ECE, The University of New Mexico, Albuquerque, NM, 87131, United States

Abstract

Animal studies indicate that different functional networks (FNs), each with a unique timecourse, may overlap at common brain regions. For understanding how different FNs overlap in the human brain and how the timecourses of overlapping FNs are modulated by cognitive tasks, we applied spatial independent component analysis (sICA) to functional magnetic resonance imaging (fMRI) data. These data were acquired from healthy participants while they performed a visual task with parametric loads of attention and working memory. SICA identified a total of 14 FNs, and they showed different extents of overlap at a majority of brain regions exhibiting any functional activity. More FNs overlapped at the higher-order association cortex including the anterior and posterior cingulate, precuneus, insula, and lateral and medial frontoparietal cortex (FPC) than at the primary sensorimotor cortex. Furthermore, overlapping FNs exhibited concurrent but different task-related modulations of timecourses. FNs showing task-related up- vs. down-modulation of timecourses overlapped at both the lateral and medial FPC and subcortical structures including the thalamus, striatum, and midbrain ventral tegmental area (VTA). Such task-related, concurrent, but opposite changes in timecourses in the same brain regions may not be detected by current analyses based on General-Linear-Model (GLM). The present findings indicate that multiple cognitive

[*]Corresponding Author: Jiansong Xu, 1 Church St., Room 729, New Haven, CT 06519, USA; Jiansong.xu@yale.edu, Tel: 203-785-5306.

All authors declare no conflict of interest with the content of this manuscript.

processes may associate with common brain regions and exhibit simultaneous but different modulations in timecourses during cognitive tasks.

Keywords

fMRI; neuroimaging; attention; working memory; cognitive function; Independent Component Analysis

Introduction

Anatomical and electrophysiological studies from animal brain indicate that multiple neural circuits, each with unique timecourse of functional activities, co-exist within the same cortical regions (Brecht 2007; Lubke & Feldmeyer 2007; Quintana & Fuster 1999; Verduzco-Flores et al 2009). Therefore, it is predicted that different functional networks (FNs) with different timecourses may overlap with each other in the human brain (Fuster 2009; Quintana & Fuster 1999; Verduzco-Flores et al 2009). The knowledge of how different FNs overlap and how the timecourses of overlapping FNs are modulated by cognitive tasks are critical for understanding brain functional organization. However, studies employing modern neuroimaging methods, such as functional magnetic resonance imaging (fMRI), usually try to associate different brain functions with different brain regions (i.e., functional parcellation scheme) without considering potential overlap of different FNs, partially due to their limited temporal and/or spatial resolutions.

With the growing interest in understanding FNs and functional connectivity, researchers have recently started to assess FN overlaps by using different approaches. For example, an approach termed Connected Iterative Scan (CIS), which is a graph-theoretic clustering algorithm that assesses FN overlap by detecting the involvement of the same functional clusters in different FNs, was applied to an fMRI dataset acquired at resting condition (Yan et al 2011). Analyses suggested that the default mode network (DMN) overlaps with the task-positive network at the posterior-cingulate and lateral parietal cortices. In another study, the combination of temporal and spatial independent component analysis (sICA) was used to analyze fMRI data acquired at rest using a high-speed scanning protocol (i.e., 0.8 s per volume) (Smith et al 2012). The results suggested that the DMN consists of multiple overlapping sub-networks. In the present study, we assessed FN overlap by applying sICA to an fMRI dataset acquired during an attention task.

SICA: 1) assumes fMRI signal from each voxel represents a linear mixture of source signals; 2) separates this signal mixture into spatially independent source signals using higher-order statistics; and 3) groups all brain regions showing synchronized source signals into independent components (ICs) (Calhoun et al 2002a; Calhoun et al 2009; McKeown et al 1998a; McKeown & Sejnowski 1998). Therefore, all brain regions associated with an IC can be treated as an intrinsically coherent FN with a unique timecourse. Any brain regions generating more than one source signal associate with more than one IC with different timecourses, and thus two or more FNs overlap at these brain regions. It is important to note that the constraint of spatially independence of ICs generated by sICA does not mean different ICs cannot overlap with each other in space. It actually means that the spatial patterns (i.e., spatial distributions in the brain) of different ICs independent from each other (Beckmann 2012; McKeown et al 1998b). However, this feature of sICA may constrain the spatial extent of FN overlap; i.e., the overlap extent revealed by sICA may be smaller than the extent discovered by temporal ICA (Calhoun et al 2012; Smith et al 2012). Therefore, the degree of FN overlap revealed by sICA may represent an underestimate.

Previous studies have demonstrated the capacity of sICA to assess FN overlap, although most of these studies do not explicitly investigate this issue. For example, McKeown et al found that most voxels contributed to 1 ~ 6 ICs (mean = 3.2) (McKeown et al 1998b). This finding indicates that as many as six FNs share common brain regions. Calhoun et al showed overlaps of several FNs in the prefrontal cortex (Calhoun et al 2002b), and each of them showed different task-related modulation of timecourse. Recent ICA studies demonstrate that the brain persistently organizes its intrinsic activity into multiple FNs both at rest and during task performance (Beckmann et al 2005; Calhoun et al 2008; Fair et al 2010; Zhang & Li 2012). Some of these FNs cover common, overlapping brain regions (Calhoun et al 2008; Kim et al 2009b; Leech et al 2011; Seeley et al 2007; Vincent et al 2008; Zhang & Raichle 2010; Zhang & Li 2012). For example, the dorsal attention network (DAN), left frontoparietal networks (LFPN), and right frontoparietal network (RFPN) subsume both lateral and medial frontoparietal cortex (FPC) (Calhoun et al 2008; Seeley et al 2007; Vincent et al 2008; Zhang & Raichle 2010; Zhang & Li 2012). Taken together, these studies demonstrate that sICA can reveal FN overlaps.

This study applied sICA to fMRI data acquired from healthy participants while they performed a visual target identification task with parametric loads of attention and working memory. The specific aims were to assess: 1) which brain regions associated with multiple FNs, and 2) how the timecourses of overlapping FNs were modulated by the task. We hypothesized that multiple FNs would overlap at higher associative cortical regions such as the FPC, and that the timecourses of overlapping FNs would show concurrent but different task-related modulations.

Materials and Methods

Participants

Data were acquired from 28 healthy participants (ages 23 – 41 years, all right handed, 13 females) recruited from the community of the University of California Los Angeles (UCLA) as described previously (Xu et al 2011). All participants gave written informed consent to participate in this study, which was approved by the Institutional Review Board at the UCLA.

Task Stimuli

The task is similar to the visual task used in a recent publication (Xu et al 2011). It uses 16 schematic faces as relevant stimuli and 64 scene pictures as background distractors (Fig. 1). Faces were composed from different combinations of five facial features (shape of face, eyes, nose, and mouth, and face color). Each facial feature had two different forms (i.e., shapes: round and oval; colors: yellow and blue). No single face was completely unique in all facial features from other faces in the group, so that each face always shared one or more features with other faces.

Task Design

The task used a block design. Stimuli for each task condition were grouped into blocks with the same 16 faces used in every trial block. These 16 faces, each paired with a scene picture, were presented one by one in a random sequence within each block. Each image was presented once for 200ms in each block, the inter-stimulus interval (ISI) was 1.0s, and the duration of each block was 19.2s (16 × 1.2s). The instruction, “Please identify,” was presented for 5s before each task block above an instruction image specifying the facial features for the targets in the following task block (Fig. 1). Participants were required to identify targets specified for each block and to respond by pressing a button as soon as possible after detecting a target. There were four targets randomly positioned in the

presentation sequence in each block, and no two targets appeared on consecutive trials. For the rest block (see below), the instruction was, “Please rest and look at the screen”.

The task has four block conditions, one for rest (L0) and the remaining three for low (L1), medium (L2), and high (L3) levels of attention and working memory load. At L0, participants were instructed to rest and look at the screen while 16 face-scene pairs were presented one by one in sequence during the presentation block. At L1, any round face with yellow color or oval face with blue color was a target. At L2, any round face with blue color and elongated nose or oval face with yellow color and round nose was a target. At L3, any round face with blue color, oval eyes and a straight mouth or oval face with yellow color, round eyes and an oval mouth was a target. Therefore, participants needed to remember and search two, three, and four facial features in conjunction to identify targets during the presentation blocks for L1, L2, and L3, respectively. We expected that from L1 to L3 the task would demand linearly increased attention and working memory for successful task performance.

Four different scripts were prepared for the task. Within each script, each block condition was repeated four times and the order of conditions was randomized. The whole script lasted for 387.2s. Each task condition within one script (i.e., 4 blocks) consisted of 64 stimuli (i.e., 16 × 4), and each of them had a different scene picture. The same 64 scene pictures were used for the four different task conditions. Stimulus presentation was implemented with Psychtoolbox (http://psychtoolbox.org/PTB-2/osx.html) and displayed on the screen of a Macintosh laptop.

Imaging Data Acquisition and Analysis

Functional images were acquired using gradient-echo EPI scanning sequence (TR/TE=1500/30ms, Flip angle=70°, 26 slices, 3mm thick with 1.2mm skip, 3.125 × 3.125 mm^2 in plane pixels) with a Siemens Allegra 3T system. The scanning plane was off the AC-PC line rostrally at 20°. The thin scanning slice and tilted scanning plane were used to reduce susceptibility-related signal loss at the basal forebrain (Deichmann et al 2003). Each participant had three functional runs, and each run used a different task script and acquired 258 volumes. The order of scripts was counterbalanced across participants.

ICA procedures

Each BOLD time series was motion-corrected, normalized to the MNI (Montreal Neurological Institute) template, and smoothed with a 5-mm kernel using FMRIB’s Software Library (FSL 4.1.4 (Smith et al 2004; Woolrich et al 2009)). Group ICA algorithm (GIFT, http://icatb.sourceforge.net/, version1.3h) was used to extract spatially independent components (ICs) (Calhoun et al 2001; Calhoun et al 2009). Data from all participants were concatenated into a single dataset and reduced using two stages of principal component analysis (PCA) (Calhoun et al 2001). The optimal number of ICs in the dataset was 23 as estimated by the minimum length description (MLD) criteria implemented in GIFT (Li et al 2007). Accordingly, 23 ICs were acquired by using Infomax algorithm to decompose the data from all subjects (Bell & Sejnowski 1995). Infomax algorithm generated a spatial map and a timecourse of the BOLD signal changes for each IC. This analysis was repeated 50 times using ICASSO for assessing the repeatability of ICs (Himberg et al 2004) (Supplemental Fig 1). Finally, IC timecourses and spatial maps were back-reconstructed for each participant (Calhoun et al 2001; Meda et al 2009).

A systematic procedure was used to diagnose artifacts and FNs. We used the probabilistic maps of white matter (WM), cerebrospinal fluid (CSF), and gray matter (GM) in MNI space provided with SPM5 (Statistical Parametric Mapping, Welcome Department of Cognitive

Neurology, London) as templates, and Multiple Linear Regression (MLR) implemented in the spatial sorting function of GIFT to compare the spatial pattern of each IC with these templates. This analysis generated three correlation coefficients (r^2) for every IC, one for each template. Any ICs showing high correlations with CSF or WM were labeled as artifacts. The threshold was set at $r^2>.05$ based on previous publications (Kim et al 2009; Zhang & Li 2012). Seven ICs (IC3, 13–15, 17, 20, 22) showed high correlations with CSF, and one (IC23) with WM. All of them showed low correlations with GM ($r^2<.05$) and therefore were diagnosed as artifacts. IC21 was also labeled as artifact because it showed a very low correlation with GM ($r^2<.001$), even though it did not show high correlations with CSF or WM. These nine ICs were excluded from further analysis. The artifacts appeared to due to head motion, eye movement, ventricular pulsations, or other causes. The remaining 14 ICs (IC1, 2, 4–12, 16, 18, 19) showed low correlations with CSF and WM and high correlations with GM, and were labeled as FNs for further analyses.

For defining significant brain regions associated with each IC, we normalized back-reconstructed spatial maps of each IC into z-scores (Beckmann et al 2005). The z-score of each voxel within a spatial map reflects its contribution to the associated timecourse. The normalized spatial maps of z-scores of each participant were averaged together across the three runs, and the averaged maps of z-scores were entered into second-level random effect analysis (one-sample t test). Therefore, a group level t-map was generated for each IC, and this t-map was used to identify the brain regions involved in the corresponding IC. The significance threshold was set at voxel height $p<.001$, False-Discovery-Rate (FDR)-corrected for multiple comparisons of voxel-wise whole-brain analysis (equivalent to $t>4.2$), and in conjunction with $k>5$ (where k indicates the voxel cluster extent). Supplementary Fig. 2 and Table 1 show the spatial distribution of 14 ICs.

Assessing FN overlap

Since each IC has a positive and a negative component, the above-described t-map of each IC contains significant clusters with positive and negative t values. In this paper, we call the positive and negative clusters in the t-map as positive and negative sub-networks, respectively, and each sub-network represents one FN. We used xjview (http://www.alivelearn.net/xjview8/) to convert each sub-network into a binary mask. Only significant voxels in each sub-network surviving the statistical threshold described above were converted into voxels with a value of one in the output mask, while all other voxels were converted into voxels with values of zero. Two masks were generated for each t-map: one for positive clusters and one for negative clusters. Twenty-eight masks, each representing one FN, were thus generated for 14 ICs. The 28 masks were added together for assessing FN overlap. Within the output map, any voxels with a value of two or higher indicate that two or more sub-networks (i.e., FNs) share this voxel, i.e., overlap at this voxel. The total number of voxels with a value equal to or greater than a specific number indicated the total volumes of overlapping regions of the specified number of FNs. For example, the total number of voxels with a value of two or greater indicated the total volumes of brain regions covered by two or more FNs.

Assessing task-related modulation over timecourses

To examine task engagement of each IC, a design matrix for each participant was constructed using SPM5. This design matrix represents the onset of each task block, convolved with a box-car hemodynamic response function. The five-second instruction period before each block was modeled implicitly as task baseline. The temporal sorting function from GIFT was used to perform a multiple regression analysis between IC timecourse and the design matrix of each participant. For each IC, this regression generated four beta-weight values for each functional run, one for each task condition (i.e., L0, L1, L2,

and L3). These beta-weight values represent the correlations between IC timecourses and the canonical hemodynamic response model of task conditions, and index the engagement of FNs during specific task conditions (Meda et al 2009). An increase or decrease in beta-weight values at one task condition relative to another indicates an increase or decrease in task-related activity in the IC.

The beta-weights of each IC for each task condition across three runs of each subject were averaged, and then the group means of averaged beta-weights for each task condition were tested against zero using SPSS one-sample t-tests. A positive beta-weight significantly different from zero indicates a task-related up-modulation of timecourse or increase in activity of the IC during a specific task condition relative to the baseline condition (i.e., task instruction), and a significant negative beta-weight indicates a task-related down-modulation of timecourse or decrease in activity of the IC. The SPSS general linear model (GLM) for repeated measures was used to assess the main effects of task loads on the beta-weight. Significant task-load-related linear changes in beta-weights were interpreted as task-load-related linear changes in activity in related ICs. The significance threshold was $p<.01$. Since the positive and negative sub-networks of each IC showed opposite timecourses and opposite task-related modulations, the positive sub-network of any IC with significant positive values of beta-weight was termed a task-positive FN, while the negative sub-network was termed a task-negative FN. The positive sub-network of any IC with significant negative values of beta-weight was termed a task-negative FN, while the negative subnetwork was termed a task-positive FN. Supplementary Table 2 shows the group mean beta-weight of each IC at each task condition.

Assessing task-related changes in activity using SPM5

We used SPM5, a GLM-based analysis, to assess task-related changes in brain activity. We used the same SPM5 design matrix created for temporal sorting as described above for this analysis. For the first level analysis of each subject, we used contrast [−3 −1 1 3] to assess significant linear changes in BOLD signal of each participant as task load increased from L0 to L1, L2, and L3. The con image generated from this contrast of each participant was inputted into a second-level (random-effect) one-sample t-test. We employed cluster $p<.05$, family-wise-error (FWE) corrected in conjunction with voxel height threshold $p<.01$ to identify task-related significant changes in BOLD signal.

Results

Task performance

The means of target hits, commission errors, and reaction times (RTs) at L1 were 94.6% (standard deviation, SD=5.1), 2.3% (SD=2.5), and 591.3ms (SD=52.2), respectively (Fig. 2). The target hits linearly decreased while the commission errors and RTs linearly increased as task load increased from L1 to L3, suggesting linearly increasing demands on attention and working memory. These behavioral data did not show significant correlations with the beta weights of any ICs after correction for multiple comparisons.

Consistent with previous described ICs

The 14 identified ICs showed high stability as indicated by repeated analyses using ICASSO (all stability indices>.94, Supplementary Fig. 1). The spatial pattern of most of 14 ICs were similar to previously described ICs generated by sICA from fMRI data acquired either at rest (Beckmann et al 2005; Raichle 2011) or during the performance of cognitive tasks (Calhoun et al 2008; Domagalik et al 2012; St Jacques et al 2011; Zhang & Li 2012) (for all ICs please see supplementary Fig. 2 and Table 1). For example, the spatial patterns of ICs 2, 5, 6, and 12 were similar to the spatial patterns of the LFPN, RFPN, sensorimotor network,

DAN, respectively, ICs 1, 7, 10, and 11 to the medial visual network, anterior portion of the default mode network (DMN), lateral visual network, and posterior portion of the DMN, respectively, and ICs 4, 8, and 16 to the insula, temporal, and saliency networks, respectively (Beckmann et al 2005; Calhoun et al 2008; Fair et al 2010; Leech et al 2011; Seeley et al 2007; Zhang & Li 2012).

Overlap of all FNs

The 28 FNs from 14 ICs together occupy 125920 voxels, which cover most cortical and subcortical regions. The majority (78.2%) of this extensive region showed overlap of two or more FNs, with a maximum overlap of 10 FNs at the dorsal anterior cingulate gyrus (ACC) (Fig. 3 and Supplementary table 3). The medial superior frontal gyrus (mSFG), posterior cingulate (PCC)/precuneus, insula and adjacent inferior frontal gyrus (IFG), middle and superior temporal gyrus (MTG & STG), superior and inferior parietal lobules showed overlap of 7 FNs, while the middle frontal gyrus (MFG), thalamus, and striatum showed overlap of 5 FNs. A general trend is that the higher-order association cortex showed overlap of more FNs than did the primary sensorimotor cortex.

Overlap of task-positive FNs

ICs 12, 18, and 19 showed significant load-dependent linear increases in beta-weight values (Fig. 4, 7, supplementary Fig. 2, 3 and table 2). Therefore, their positive sub-networks showed load-dependent increases in activity and were task-positive FNs. ICs 2, 4, 7, 8, and 9, showed significant load-dependent linear decreases in beta-weights (Fig. 5, 7, supplementary Fig. 2, 3 and table 2). Therefore, their negative sub-networks showed load-dependent increases in activity and were task-positive FNs. Beta-weights of ICs 5, 6, 10, and 11 were significantly negative at one or more task conditions even though they did not show significant load-dependent linear changes. Therefore, their negative subnetworks showed increases in activity at one or more task conditions and were task-positive FNs. Therefore, there are 12 task-positive FNs, and they occupy extensive cortical and subcortical regions (a total of 67712 voxels). These task-positive FNs showed extensive overlap (Fig. 4 and supplementary table 4). The dorsal ACC showed overlap of 5 FNs, while the bilateral insula and inferior parietal lobule showed overlap of 4 FNs. The medial and lateral prefrontal cortex (PFC) and superior parietal lobule, thalamus, and striatum showed overlap of 2 ~ 3 FNs.

Overlap of task-negative FNs

Using the same logic as described in the above section, the negative subnetworks of ICs 12, 18, 19 and the positive sub-networks of ICs 2, 4, 5, 6, 7, 8, 9, 10, and 11 were task-negative FNs. The 12 task-negative FNs together occupied extensive cortical and subcortical regions (a total of 111937 voxels). These task-negative FNs showed extensive overlap (Fig. 5, 7 and supplementary table 5). The bilateral STG showed overlap of 6 task-negative FNs, while the medial SFG and precuneus/PCC showed overlap of 5 FNs. Perigenual ACC, IFG, inferior parietal lobule, and thalamus showed overlap of 3 ~ 4 FNs.

Overlap of task-positive and negative FNs

The task-positive and task-negative FNs overlap extensively (Fig. 6). The overlapping areas cover 58638 voxels, about 86.6% and 52.4% of the total volumes covered by task-positive and negative FNs, respectively. They include the medial and lateral frontoparietal cortex (FPC), insula, temporal cortex, and subcortical structures such as the thalamus, striatum, and midbrain ventral tegmental area (VTA).

As described above, ICs 2, 5, and 12 were similar to the LFPN, RFPN, and DAN in spatial patterns, and the positive sub-networks of ICs 2 and 5 were task-negative FNs, while the positive sub-network of IC12 was a task-positive FN (Fig. 7 and supplementary Fig. 2, 3). These task-positive and negative FNs overlapped at the medial and lateral FPC, ACC, insula, intraparietal sulcus, precuneus/PCC, thalamus, and caudate (Fig. 7 and supplementary table 6).

Task-related activity revealed by SPM5

The present finding of overlap of task-positive and task-negative FNs raises the question of whether concurrent, opposite changes of source signals in the same brain regions prevent GLM-based analysis from detecting task-related changes in BOLD signal because opposite changes in source signals may cancel out each other. To answer this question, we used SPM5 to analyze load-dependent changes in BOLD signal in the original dataset. Several regions including the lateral PFC, pre-supplementary motor cortex, insula, and parietal lobules showed load-dependent linear increase in BOLD signal (Fig. 8, Supplementary Table 7). Their total volume is 8055 voxels, about 11.9% of the total volume of the 12 task-positive FNs generated by sICA. In addition, several regions including the medial FPC, insula, and tempoparietal junction showed load-dependent linear decreases in BOLD signal (Fig 8, Supplementary Table 7). Their total volume is 29356 voxels, about 26.2% of the total volume of the 12 task-negative FNs generated by sICA.

Discussion

Recent studies have used sICA to extract FNs from BOLD (blood-oxygen-level-dependent) time series acquired during resting conditions and report that about 10 FNs show consistent spatial patterns across different populations and studies (Beckmann et al 2005; Calhoun et al 2008; Smith et al 2009; Zhang & Raichle 2010). These FNs maintain their general spatial patterns during cognitive tasks demanding attention, working memory, and/or response inhibition, while showing more or less task-related modulations including changes in spatial extent and strength of internal functional connectivity (Calhoun et al 2008; Domagalik et al 2012; Esposito et al 2009; Esposito et al 2005; Smith et al 2009; St Jacques et al 2011; Zhang & Raichle 2010). The current study extracted 14 ICs from fMRI data acquired from healthy participants performing an attention task. Most of these ICs showed spatial patterns consistent with reported ICs generated by sICA and fMRI data acquired either during rest or task performance. Here, “consistent” spatial pattern means that the corresponding ICs identified in different studies involve common key brain regions, and does not mean that these ICs are exactly identical (Domagalik et al 2012). The consistent findings from the present and previous studies suggest that our sICA identified appropriately networks existing in healthy participants.

The current study generated multiple important findings by assessing the overlap of extracted FNs and task-load-related modulations of the timecourses of overlapping FNs. First, a majority (78.2%) of brain regions associated with any FN showed overlap of two or more FNs. This finding is in line with other data indicating that most voxels contribute to several ICs (mean = 3.2) (McKeown et al 1998b) and that different FNs overlap at common regions (Domagalik et al 2012; Menz et al 2009; St Jacques et al 2011; van Wageningen et al 2009; Wu et al 2009). Since different FNs show different timecourses during task performance and probably associate with different cognitive processes, we interpret the finding of FN overlaps as indications of the same brain regions being simultaneously involved in multiple cognitive processes, consistent with previous interpretations of FN overlap (Menz et al 2009; van Wageningen et al 2009; Wu et al 2009). This interpretation is also consistent with the data of different tasks activating the same brain regions at different times as reported from fMRI studies using GLM-based analyses (Burgess et al 2007;

Duncan 2010; Duncan & Owen 2000; Gilbert et al 2006). However, the data derived from sICA demonstrate that the same neural substrates can contribute to multiple cognitive processes concurrently, in addition to sequentially as demonstrated by GLM-based analyses.

Second, we found that more FNs overlapped at the higher-order association cortex, especially the ACC, medial SFG, precuneus/PCC, IFG, superior and middle temporal gyrus, and superior and inferior parietal lobules, than at the primary sensorimotor cortex. This finding supports our first hypothesis and suggests that more FNs operate concurrently in the higher-order association cortex than in the primary sensorimotor cortex. This finding is consistent with the data that the higher-order association cortex, as compared to the primary sensorimotor cortex, is functionally more complex and has a greater density of functional connectivity (Buckner et al 2009; Mesulam 1998; Tomasi & Volkow 2011). Since the FNs extracted from fMRI data of resting condition vs. task performance are quite similar in their general spatial patterns as discussed above, we predict similar overlap should exist among FNs extracted from resting data. However, we cannot directly test this at present because we did not acquire resting fMRI data from these participants. Several recent studies used seed-based approaches to assess functional connectivity and reported extensive overlaps of multiple FNs (Buckner et al 2009; Fox et al 2005; Tomasi & Volkow 2011). However, these findings are different from the current finding in that the seed-based approach does not separate the BOLD signal mixture from each voxel into source signals. The FN overlap reported in these studies may reflect the phenomenon of the timecourse of BOLD signal in one region significantly correlating with the timecourses of two or more other regions, while the timecourses of the other regions do not significantly correlate with each other. However, the overlaps found in the current study reflect the timecourses of different source signals from common brain regions correlating with the timecourses of different source signals from other brain regions.

Third, we found that task-positive and task-negative FNs share extensive regions including both the lateral and medial frontoparietal cortex (FPC), supporting our second hypothesis. This finding provides direct support to the hypothesis that FNs of different timecourses overlap with each other in the FPC, consistent with data from animal studies (Fuster 2009). This finding is also consistent with the data indicating overlaps of task-positive and task-negative FNs as revealed by Connected Iterative Scan (CIS) (Yan et al 2011). The lateral and medial FPCs often show opposite changes in BOLD signal during cognitive tasks. The lateral FPC has been demonstrated to associate with cognitive control such as attention and working memory, whereas the medial FPC is hypothesized to be a component of the default-mode network (DMN) and to associate with intrinsically generated, task-independent mental activity such as task-unrelated thought (Fox et al 2005; Sonuga-Barke & Castellanos 2007). However, other evidence indicates that the medial FPC, the core of DMN (Buckner et al 2009), also contributes to working memory. For example, lesions of the medial prefrontal cortex (PFC) may impair working memory (Barbey et al 2011; Szatkowska et al 2011; Tsuchida & Fellows 2009); working memory performance has been correlated with the strength of functional connectivity within DMN, especially between the medial PFC and the posterior cingulate (PCC)/precuneus, even though these regions show task-related decreases in BOLD signal (Hampson et al 2006); and the dorsal and ventral PCC/precuneus show opposite changes (increases vs. decreases) in functional connectivity with other DMN regions during a high- (2-back) relative to a low-demanding (0-back) working memory task (Leech et al 2011). The current finding, together with the CIS data (Yan et al 2011), suggests that there may be no sharp border between neural substrates associated with cognitive control vs. task-unrelated thoughts, and that these neural substrates may intermix with each other at both lateral and medial PFC. However, the lateral PFC may predominantly associate with cognitive control, and therefore show a net increase in the BOLD signal mixture during working-memory-task performance even though some of its

neural substrates associate with task-unrelated thoughts. The medial PFC may predominantly associate with task-unrelated thoughts, and therefore show a net decrease in the BOLD signal mixture during working-memory-task performance even though some of its neural substrates associate with working memory. The overlaps of task-positive and task-negative FNs raise the question of how different sets of multiple FNs at different voxels impact FNs identified by commonly used seed-based approaches.

Fourth, we found load-dependent, opposite (up vs. down) modulations of ICs 2, 5, and 12, even though they share common cortical regions at both the lateral and medial FPC. The spatial pattern of IC12 is consistent with the DAN, and ICs 2 and 5 are consistent with the LFPN and RFPN, respectively (Leech et al 2011; Zhang & Raichle 2010). The DAN, LFPN, and RFPN are observed regularly in functional connectivity studies using either sICA or seed-based approaches (Cole et al 2010; Leech et al 2011; Zhang & Raichle 2010; Zhang & Li 2012). In the current study, the DAN, along with several other FNs, showed load-dependent linear increases in *positive* modulation, and thus may contribute to top-down attentional control during task performance. The LFPN together with several other FNs showed load-dependent linear increases in *negative* modulation, indicating that its activity might interfere with top-down attentional control and need to be suppressed. Even though the RFPN did not show significant load-dependent modulation, it showed negative modulation during the L2 attentional load condition, and therefore its activity was suppressed at L2. In a recent ICA study using a stop-signal task, both LFPN and RFPN showed negative modulations for go trials and positive modulations for successful stop trials, but they showed opposite modulations for failed stop trials (Zhang & Li 2012). The DAN (shown in the supplementary materials of (Zhang & Li 2012) as IC16) showed modulations opposite to those shown by LFPN and RFPN; i.e., positive modulation for go-trials and negative modulation for successful stop-trials. Furthermore, the LFPN showed up-modulation during a working memory task in another study (Kim et al 2009a). These data demonstrate that the DAN, LFPN, and RFPN associate with different aspects of cognitive control, although they share extensive common regions in the FPC. Their opposite task-related modulations indicate that task-related deactivation is not restricted to the DMN (i.e., neural substrates associated with intrinsically generated task-unrelated thought).

Finally, we found that relative to sICA, SPM5, utilizing a GLM-based analysis, identified much smaller volumes of brain regions exhibiting task-related increases and decreases in activity. This finding is consistent with previous data in which sICA implicated more voxels and larger regions in task-related activities than did GLM-based analyses (Domagalik et al 2012; Kim et al 2011; Malinen et al 2007; Tie et al 2008). The opposite changes in source signals from the same voxels as revealed by sICA probably contribute to this difference between sICA and GLM-based analyses. Furthermore, sICA is identifying components which are temporally coherent (i.e. show functional connectivity) whereas the GLM is focused on identifying voxels that are modulated by a task, but which may not be correlated with one another. These very different approaches likely contribute to their different findings. Therefore, the absence of task-related changes in BOLD signal mixture as assessed by GLM-based analyses does not necessary equate to the absence of task-related activity. These findings suggest that GLM-based analyses should be regularly supplemented by sICA or other approaches capable of differentiating BOLD signal mixture into source signals to identify task-related changes in brain activation.

This study extracted ICs using sICA, which has several limitations. First, the spatial pattern of each IC may be different dependent on different number of ICs extracted (Esposito & Goebel 2011). Therefore, the numbers and locations of FN overlap may change for different numbers of extracted ICs. However, it has been demonstrated that ICs remain accurate for a large range of numbers of ICs (Esposito & Goebel 2011). Second, there is no reliable

method to accurately identify which IC represents true source signal and which IC represents artifacts generated by ICA. However, many ICs generated by sICA and fMRI data are very consistent in spatial patterns across different studies and populations (Calhoun et al 2008; Domagalik et al 2012; Raichle 2011). Finally, the imaging resolution, i.e., voxel size, may affect the spatial extent of overlap. Smaller voxel volume may reduce the partial volume effect and thus alter the overlap extent.

In summary, this study demonstrates FN overlaps by using sICA to separate signal mixtures from the same brain regions into source signals. The overlapping FNs show concurrent but idiosyncratic modulations of activity during an attentional task. The current GLM-based analysis cannot detect FN overlaps because it cannot segregate the signal mixture from each voxel into source signals. For a better understanding of brain functional organization methods such as sICA that are capable of differentiating signal mixture should be regularly employed to supplement GLM-based analyses.

Supplementary Material

Refer to Web version on PubMed Central for supplementary material.

Acknowledgments

We thank Dr. John Wall at The University of Toledo for thoughtful comments. This study was funded by the following grants: National Institute On Drug Abuse (NIDA) grants R03 DA022364 (Xu), K01 DA027750 (Xu), K02DA026990 (Li), P20 DA027844 (Potenza).

References

Barbey AK, Koenigs M, Grafman J. Orbitofrontal contributions to human working memory. Cereb Cortex. 2011; 21:789–95. [PubMed: 20724371]

Beckmann CF. Modelling with independent components. Neuroimage. 2012; 62:891–901. [PubMed: 22369997]

Beckmann CF, DeLuca M, Devlin JT, Smith SM. Investigations into resting-state connectivity using independent component analysis. Philos Trans R Soc Lond B Biol Sci. 2005; 360:1001–13. [PubMed: 16087444]

Bell AJ, Sejnowski TJ. An information-maximization approach to blind separation and blind deconvolution. Neural Comput. 1995; 7:1129–59. [PubMed: 7584893]

Brecht M. Barrel cortex and whisker-mediated behaviors. Curr Opin Neurobiol. 2007; 17:408–16. [PubMed: 17702566]

Buckner RL, Sepulcre J, Talukdar T, Krienen FM, Liu H, et al. Cortical hubs revealed by intrinsic functional connectivity: mapping, assessment of stability, and relation to Alzheimer's disease. J Neurosci. 2009; 29:1860–73. [PubMed: 19211893]

Burgess PW, Gilbert SJ, Dumontheil I. Function and localization within rostral prefrontal cortex (area 10). Philos Trans R Soc Lond B Biol Sci. 2007; 362:887–99. [PubMed: 17403644]

Calhoun VD, Adali T, Pearlson GD, Pekar JJ. A method for making group inferences from functional MRI data using independent component analysis. Hum Brain Mapp. 2001; 14:140–51. [PubMed: 11559959]

Calhoun VD, Adali T, Pearlson GD, van Zijl PC, Pekar JJ. Independent component analysis of fMRI data in the complex domain. Magn Reson Med. 2002a; 48:180–92. [PubMed: 12111945]

Calhoun VD, Eichele T, Adali T, Allen EA. Decomposing the brain: components and modes, networks and nodes. Trends Cogn Sci. 2012; 16:255–6. [PubMed: 22487186]

Calhoun VD, Kiehl KA, Pearlson GD. Modulation of temporally coherent brain networks estimated using ICA at rest and during cognitive tasks. Hum Brain Mapp. 2008; 29:828–38. [PubMed: 18438867]

Calhoun VD, Liu J, Adali T. A review of group ICA for fMRI data and ICA for joint inference of imaging, genetic, and ERP data. Neuroimage. 2009; 45:S163–72. [PubMed: 19059344]

Calhoun VD, Pekar JJ, McGinty VB, Adali T, Watson TD, Pearlson GD. Different activation dynamics in multiple neural systems during simulated driving. Hum Brain Mapp. 2002b; 16:158–67. [PubMed: 12112769]

Cole MW, Pathak S, Schneider W. Identifying the brain's most globally connected regions. Neuroimage. 2010; 49:3132–48. [PubMed: 19909818]

Deichmann R, Gottfried JA, Hutton C, Turner R. Optimized EPI for fMRI studies of the orbitofrontal cortex. Neuroimage. 2003; 19:430. [PubMed: 12814592]

Domagalik A, Beldzik E, Fafrowicz M, Oginska H, Marek T. Neural networks related to pro-saccades and anti-saccades revealed by independent component analysis. Neuroimage. 2012; 62:1325–33. [PubMed: 22705376]

Duncan J. The multiple-demand (MD) system of the primate brain: mental programs for intelligent behaviour. Trends Cogn Sci. 2010; 14:172–9. [PubMed: 20171926]

Duncan J, Owen AM. Common regions of the human frontal lobe recruited by diverse cognitive demands. Trends in Neurosciences. 2000; 23:475. [PubMed: 11006464]

Esposito F, Aragri A, Latorre V, Popolizio T, Scarabino T, et al. Does the default-mode functional connectivity of the brain correlate with working-memory performances? Arch Ital Biol. 2009; 147:11–20. [PubMed: 19678593]

Esposito F, Goebel R. Extracting functional networks with spatial independent component analysis: the role of dimensionality, reliability and aggregation scheme. Curr Opin Neurol. 2011; 24:378–85. [PubMed: 21734575]

Esposito F, Scarabino T, Hyvarinen A, Himberg J, Formisano E, et al. Independent component analysis of fMRI group studies by self-organizing clustering. Neuroimage. 2005; 25:193–205. [PubMed: 15734355]

Fair DA, Bathula D, Mills KL, Dias TG, Blythe MS, et al. Maturing thalamocortical functional connectivity across development. Front Syst Neurosci. 2010; 4:10. [PubMed: 20514143]

Fox MD, Snyder AZ, Vincent JL, Corbetta M, Van Essen DC, Raichle ME. The human brain is intrinsically organized into dynamic, anticorrelated functional networks. Proc Natl Acad Sci U S A. 2005; 102:9673–8. [PubMed: 15976020]

Fuster JM. Cortex and memory: emergence of a new paradigm. J Cogn Neurosci. 2009; 21:2047–72. [PubMed: 19485699]

Gilbert SJ, Simons JS, Frith CD, Burgess PW. Performance-related activity in medial rostral prefrontal cortex (area 10) during low-demand tasks. J Exp Psychol Hum Percept Perform. 2006; 32:45–58. [PubMed: 16478325]

Hampson M, Driesen NR, Skudlarski P, Gore JC, Constable RT. Brain connectivity related to working memory performance. J Neurosci. 2006; 26:13338–43. [PubMed: 17182784]

Himberg J, Hyvarinen A, Esposito F. Validating the independent components of neuroimaging time series via clustering and visualization. Neuroimage. 2004; 22:1214–22. [PubMed: 15219593]

Kim DI, Manoach DS, Mathalon DH, Turner JA, Mannell M, et al. Dysregulation of working memory and default-mode networks in schizophrenia using independent component analysis, an fBIRN and MCIC study. Hum Brain Mapp. 2009a; 30:3795–811. [PubMed: 19434601]

Kim DI, Mathalon DH, Ford JM, Mannell M, Turner JA, et al. Auditory oddball deficits in schizophrenia: an independent component analysis of the fMRI multisite function BIRN study. Schizophr Bull. 2009b; 35:67–81. [PubMed: 19074498]

Kim KK, Karunanayaka P, Privitera MD, Holland SK, Szaflarski JP. Semantic association investigated with functional MRI and independent component analysis. Epilepsy Behav. 2011; 20:613–22. [PubMed: 21296027]

Leech R, Kamourieh S, Beckmann CF, Sharp DJ. Fractionating the default mode network: distinct contributions of the ventral and dorsal posterior cingulate cortex to cognitive control. J Neurosci. 2011; 31:3217–24. [PubMed: 21368033]

Li YO, Adali T, Calhoun VD. Estimating the number of independent components for functional magnetic resonance imaging data. Hum Brain Mapp. 2007; 28:1251–66. [PubMed: 17274023]

Lubke J, Feldmeyer D. Excitatory signal flow and connectivity in a cortical column: focus on barrel cortex. Brain Struct Funct. 2007; 212:3–17. [PubMed: 17717695]

Malinen S, Hlushchuk Y, Hari R. Towards natural stimulation in fMRI--issues of data analysis. Neuroimage. 2007; 35:131–9. [PubMed: 17208459]

McKeown MJ, Jung TP, Makeig S, Brown G, Kindermann SS, et al. Spatially independent activity patterns in functional MRI data during the Stroop color-naming task. Proceedings of the National Academy of Sciences of the United States of America. 1998a; 95:803. [PubMed: 9448244]

McKeown MJ, Makeig S, Brown GG, Jung TP, Kindermann SS, et al. Analysis of fMRI data by blind separation into independent spatial components. Hum Brain Mapp. 1998b; 6:160–88. [PubMed: 9673671]

McKeown MJ, Sejnowski TJ. Independent component analysis of fMRI data: examining the assumptions. Hum Brain Mapp. 1998; 6:368–72. [PubMed: 9788074]

Meda SA, Stevens MC, Folley BS, Calhoun VD, Pearlson GD. Evidence for anomalous network connectivity during working memory encoding in schizophrenia: an ICA based analysis. PLoS One. 2009; 4:e7911. [PubMed: 19936244]

Menz MM, McNamara A, Klemen J, Binkofski F. Dissociating networks of imitation. Hum Brain Mapp. 2009; 30:3339–50. [PubMed: 19350561]

Mesulam MM. From sensation to cognition. Brain. 1998; 121 (Pt 6):1013–52. [PubMed: 9648540]

Quintana J, Fuster JM. From perception to action: temporal integrative functions of prefrontal and parietal neurons. Cereb Cortex. 1999; 9:213–21. [PubMed: 10355901]

Raichle ME. The restless brain. Brain Connect. 2011; 1:3–12. [PubMed: 22432951]

Seeley WW, Menon V, Schatzberg AF, Keller J, Glover GH, et al. Dissociable intrinsic connectivity networks for salience processing and executive control. J Neurosci. 2007; 27:2349–56. [PubMed: 17329432]

Smith SM, Fox PT, Miller KL, Glahn DC, Fox PM, et al. Correspondence of the brain's functional architecture during activation and rest. Proc Natl Acad Sci U S A. 2009; 106:13040–5. [PubMed: 19620724]

Smith SM, Jenkinson M, Woolrich MW, Beckmann CF, Behrens TE, et al. Advances in functional and structural MR image analysis and implementation as FSL. Neuroimage. 2004; 23(Suppl 1):S208–19. [PubMed: 15501092]

Smith SM, Miller KL, Moeller S, Xu J, Auerbach EJ, et al. Temporally-independent functional modes of spontaneous brain activity. Proc Natl Acad Sci U S A. 2012; 109:3131–6. [PubMed: 22323591]

Sonuga-Barke EJ, Castellanos FX. Spontaneous attentional fluctuations in impaired states and pathological conditions: a neurobiological hypothesis. Neurosci Biobehav Rev. 2007; 31:977–86. [PubMed: 17445893]

St Jacques PL, Kragel PA, Rubin DC. Dynamic neural networks supporting memory retrieval. Neuroimage. 2011; 57:608–16. [PubMed: 21550407]

Szatkowska I, Szymanska O, Marchewka A, Soluch P, Rymarczyk K. Dissociable contributions of the left and right posterior medial orbitofrontal cortex in motivational control of goal-directed behavior. Neurobiol Learn Mem. 2011; 96:385–91. [PubMed: 21741492]

Tie Y, Whalen S, Suarez RO, Golby AJ. Group independent component analysis of language fMRI from word generation tasks. Neuroimage. 2008; 42:1214–25. [PubMed: 18621548]

Tomasi D, Volkow ND. Functional connectivity hubs in the human brain. Neuroimage. 2011; 57:908–17. [PubMed: 21609769]

Tsuchida A, Fellows LK. Lesion evidence that two distinct regions within prefrontal cortex are critical for n-back performance in humans. J Cogn Neurosci. 2009; 21:2263–75. [PubMed: 19199405]

van Wageningen H, Jorgensen HA, Specht K, Eichele T, Hugdahl K. The effects of the glutamate antagonist memantine on brain activation to an auditory perception task. Hum Brain Mapp. 2009; 30:3616–24. [PubMed: 19449331]

Verduzco-Flores S, Bodner M, Ermentrout B, Fuster JM, Zhou Y. Working memory cells' behavior may be explained by cross-regional networks with synaptic facilitation. PLoS One. 2009; 4:e6399. [PubMed: 19652716]

Vincent JL, Kahn I, Snyder AZ, Raichle ME, Buckner RL. Evidence for a frontoparietal control system revealed by intrinsic functional connectivity. J Neurophysiol. 2008; 100:3328–42. [PubMed: 18799601]

Woolrich MW, Jbabdi S, Patenaude B, Chappell M, Makni S, et al. Bayesian analysis of neuroimaging data in FSL. Neuroimage. 2009; 45:S173–86. [PubMed: 19059349]

Wu X, Lu J, Chen K, Long Z, Wang X, et al. Multiple neural networks supporting a semantic task: an fMRI study using independent component analysis. Neuroimage. 2009; 45:1347–58. [PubMed: 19166946]

Xu J, Monterosso J, Kober H, Balodis IM, Potenza MN. Perceptual load-dependent neural correlates of distractor interference inhibition. PLoS One. 2011; 6:e14552. [PubMed: 21267080]

Yan X, Kelley S, Goldberg M, Biswal BB. Detecting overlapped functional clusters in resting state fMRI with Connected Iterative Scan: a graph theory based clustering algorithm. J Neurosci Methods. 2011; 199:108–18. [PubMed: 21565220]

Zhang D, Raichle ME. Disease and the brain's dark energy. Nat Rev Neurol. 2010; 6:15–28. [PubMed: 20057496]

Zhang S, Li CS. Functional networks for cognitive control in a stop signal task: independent component analysis. Hum Brain Mapp. 2012; 33:89–104. [PubMed: 21365716]

Highlights

- We assessed overlap of brain functional networks (FNs) extracted by spatial ICA.
- Majority of brain functional regions showed overlap of two or more FNs.
- Higher-order association cortex showed overlap of more FNs than did the primary sensorimotor cortex.
- Overlapping FNs showed opposite modulations of activity during an attentional task.
- Multiple cognitive processes associate with common brain regions and operate concurrently.

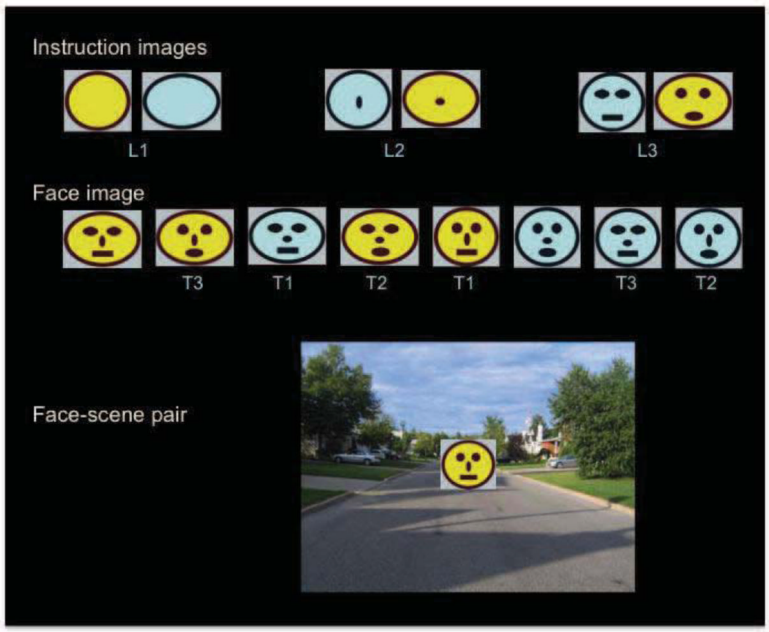

Fig 1.

Diagram demonstrating elements of the visual target identification task. The first row shows instruction images used in the instructions before the onset of each task block. L1, L2, and L3 indicate facial features for identifying targets of low (L1), medium (L2), and high (L3) load conditions, respectively. During the task, the instruction screen showed “Please Identify” above each instruction image for five seconds before the onset of the following stimuli block. For the rest condition, the instruction screen showed “Please rest and look at the screen” without any additional instruction image. The middle row shows examples of faces used in the task. T1, T2, and T3 indicate examples of targets for task conditions L1, L2, and L3, respectively. The bottom row shows an example of face-scene pairs used as stimuli in the task.

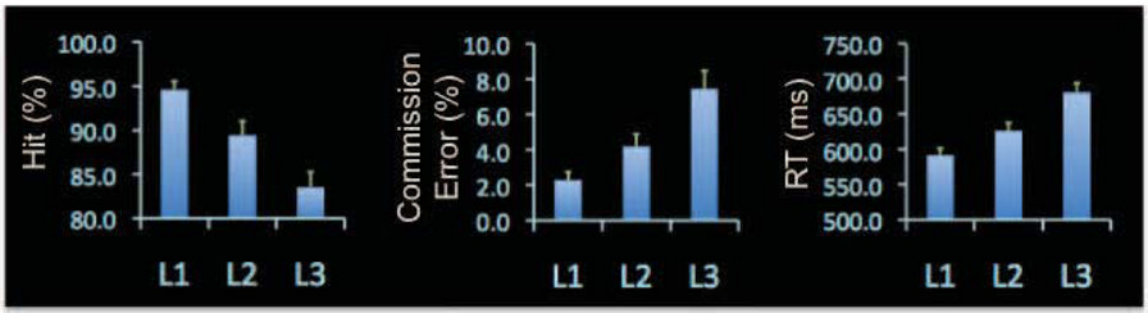

Fig 2.

Task performance. The bar graphs show the means of target hit rate, commission error rate, and reaction time (RT) (ms), respectively, at task conditions of low (L1), medium (L2), and high (L3) task load. The error bars indicate standard error (SE) of means. The SPSS general linear model for repeated measures was used to assess the effect of task load on task performance. All measures showed significant linear changes as task load increased from L1 to L2 and L3 ($p<.001$).

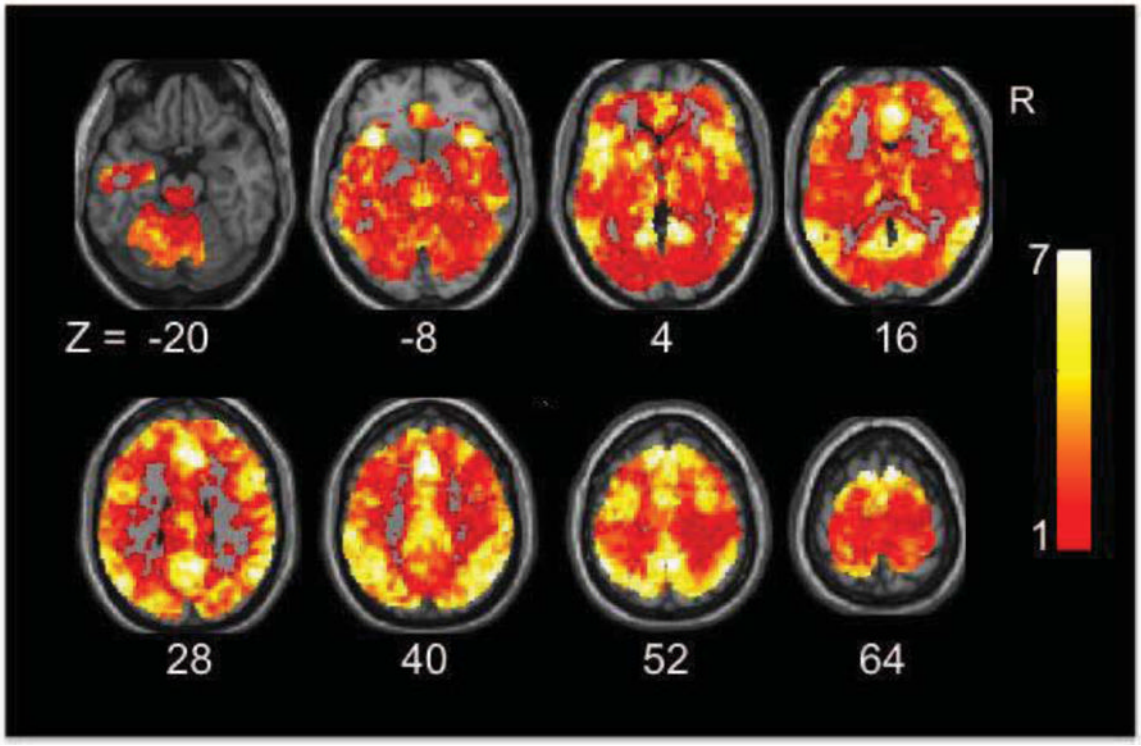

Fig 3.

Overlap of all functional networks (FNs). Yellow-red colors on the Montreal Neurological Institute (MNI) T1 templates indicate brain regions covered by one or more FNs. The color bar indicates the number of FNs. The number below each brain image indicates the Z coordinates in MNI space. Abbreviation: R: right.

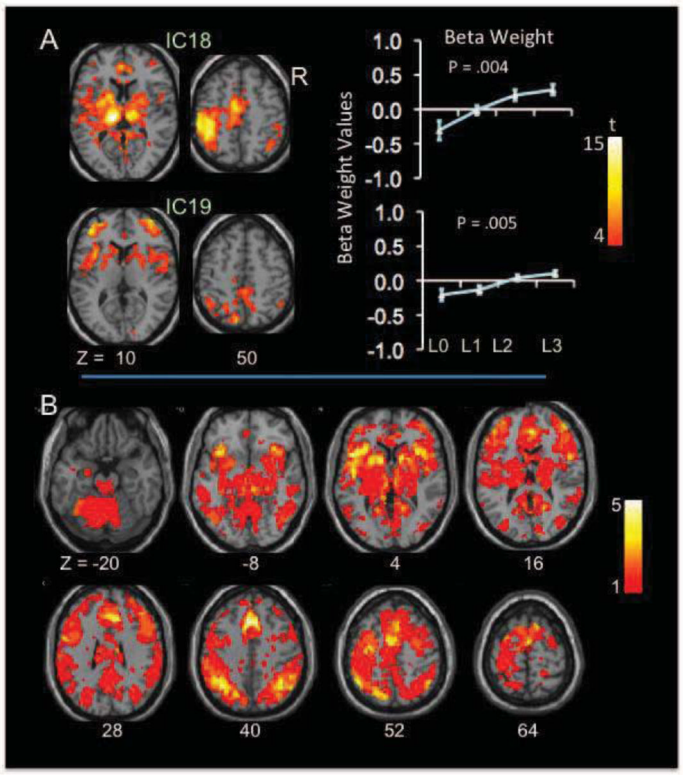

Fig 4.

Overlap of task-positive functional networks (FNs). A. Colors on the Montreal Neurological Institute (MNI) T1 templates show the spatial distribution of positive sub-networks from IC18 and 19. Only clusters surviving corrections for voxel-wise whole-brain analyses are shown. The color bar indicates t values. The “Beta-weight” column shows values of beta-weights at each task condition. Error bars indicate standard errors (SEs) of means. The p value on each panel indicates the statistical significance of task-load-related linear changes in beta-weights. B. Yellow-red colors on T1 templates indicate brain regions covered by one or more task-positive FNs. The color bar indicates the number of overlapping FNs. The number below each brain image indicates the Z coordinates in MNI space. Abbreviations: L0: rest condition; L1-3: low, medium, and high task load conditions; R: right; Z: z coordinate in MNI space.

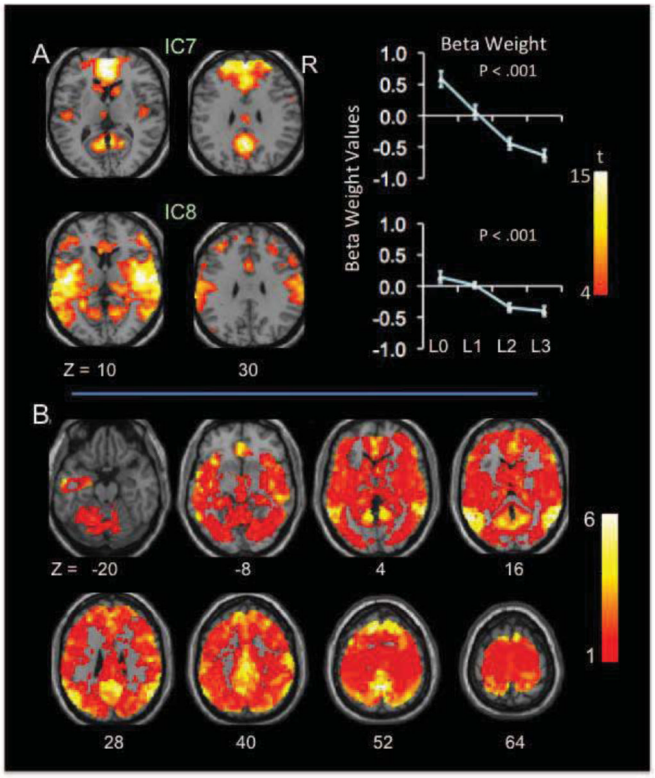

Fig 5.

Overlap of task-negative functional networks (FNs). A. Colors on the Montreal Neurological Institute (MNI) T1 templates show the spatial distribution of positive sub-networks from IC7 and 8. B. Yellow-red colors on T1 templates indicate brain regions covered by one or more task-negative FNs. Please see fig. 4 legend for additional details.

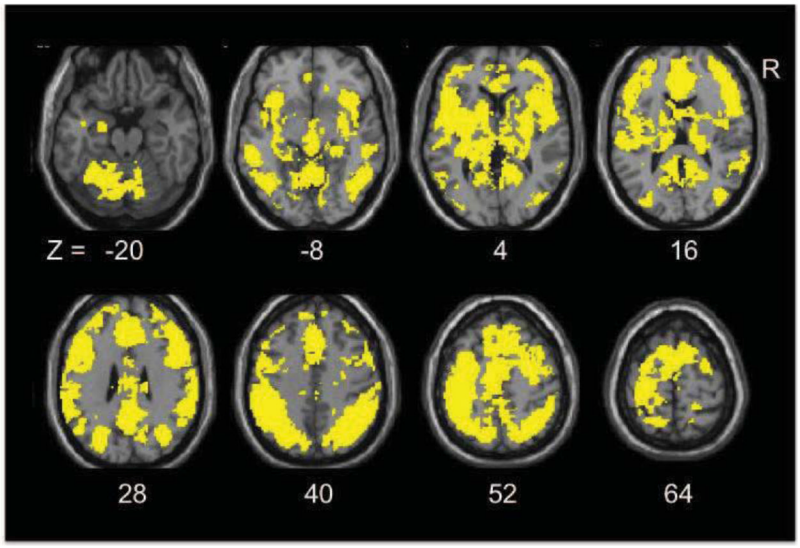

Fig 6.

Overlap of task-positive and negative functional networks (FNs). The yellow color on the Montreal Neurological Institute (MNI) T1 templates indicates brain regions covered by both task-positive and task-negative FNs. The number below each brain image indicates the Z coordinates in MNI space. Abbreviation: R: right.

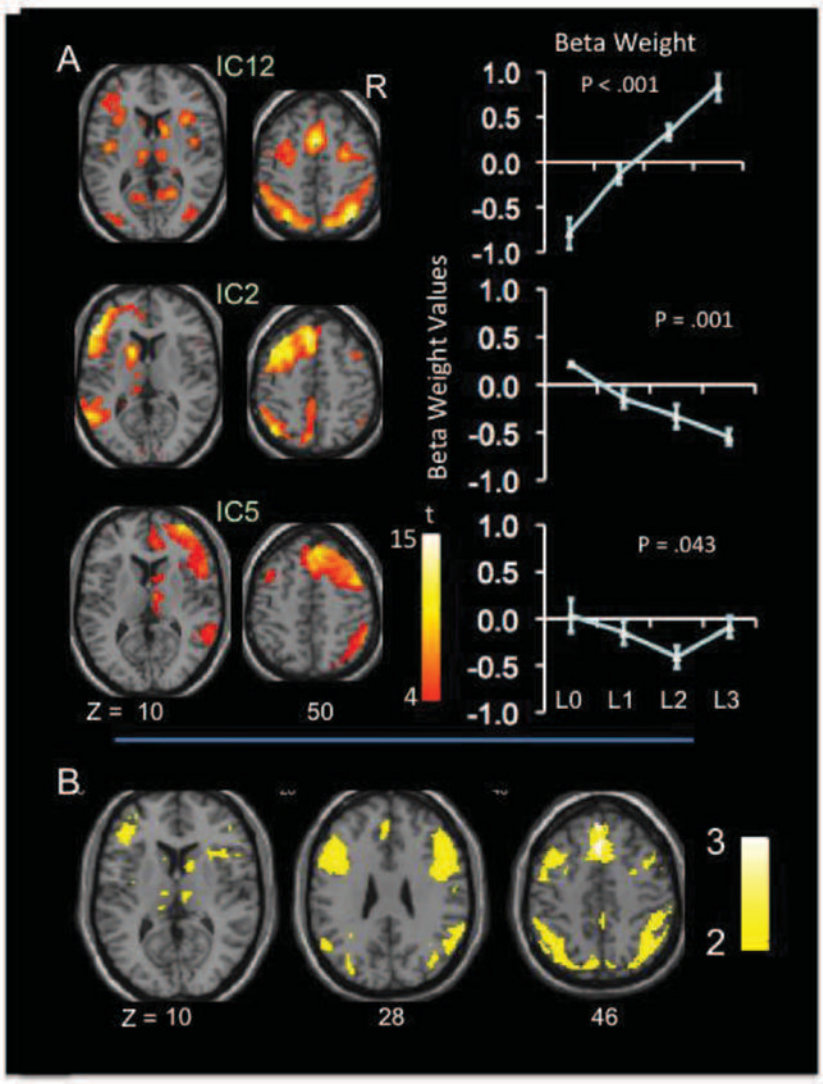

Fig. 7.

Overlap of positive sub-network of ICs 2, 5, and 12. A. Colors on the Montreal Neurological Institute (MNI) T1 template show the spatial distribution of positive sub-networks of ICs 2, 5, and 12. B. The yellow-white colors on the T1 templates indicate overlaps of positive sub-networks of ICs 2, 5, and 12. Please see fig. 4 legend for additional details.

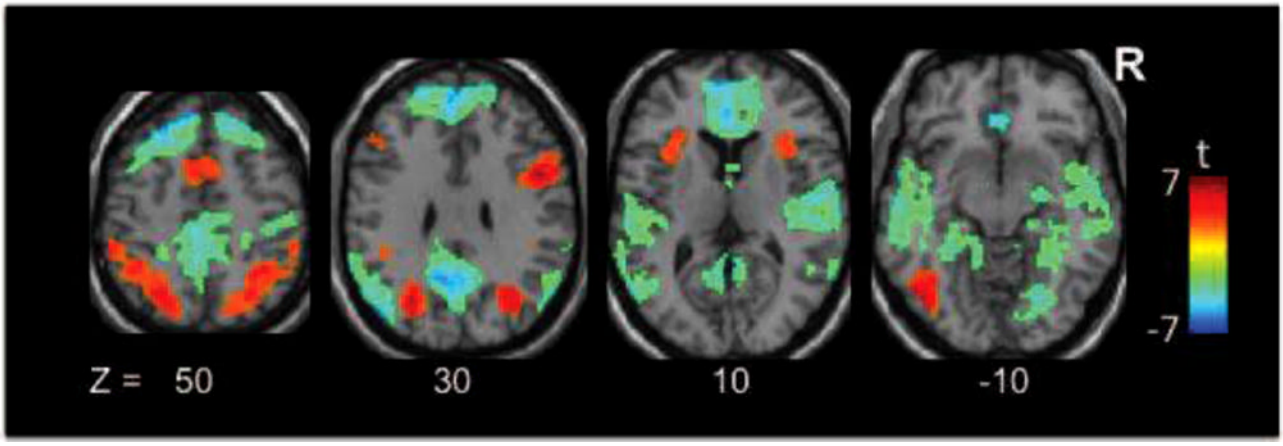

Fig. 8.

Task-load-dependent changes in BOLD signal revealed by SPM5. The colors on the T1 templates in MNI space show significant linear changes in BOLD signal as task load changed from L0 to L3 in the original dataset. The color bar indicates the t values. Only voxels surviving $p<.01$ and cluster $p<.05$, FWE-corrected for multiple comparisons of voxel-wise whole-brain analysis are shown. The number below each brain image indicates the Z coordinates in MNI space. Abbreviations: R: right hemisphere.